Journal of Structural Geology, Vol. 7, No. 6, pp. 637 to 650, 1985
Printed in Great Britain

0191-8141/85 $03.00 + 0.00

Progressive and polyphase deformation of the Schistes Lustrés in Cap Corse, Alpine Corsica†

LYAL HARRIS*

Centre Armoricain d'Etude Structurale des Socles (CNRS), Université de Rennes, 35042 Rennes Cedex, France

(*Received* 8 *February* 1984; *accepted in revised form* 25 *January* 1985)

Abstract—In Cap Corse, progressive deformation during Late Cretaceous obduction of the ophiolitic Schistes Lustrés (*sensu lato*) as a pile of imbricate, lens-shaped units during blueschist facies metamorphism was non-coaxial. Two zones are recognized: a lower series emplaced towards the west is overlain by a series emplaced towards the south–southwest in Cap Corse. Equivalent structures (differing only in orientation) occur in both zones. The change in thrust direction was responsible for local refolding and reorientation of previously formed structures, parallel to the new stretching direction immediately below the thrust contact between the two zones, and within localized shear zones in the underlying series.

Both zones are refolded about E-overturned F_2 folds trending between 350 and 025°. Local minor E-directed thrusts occur associated with the F_2 folds. This second deformation of Middle Eocene age is considered to be related to the backthrusting of an overlying klippe containing gneisses of South Alpine origin, and is followed by a third Late Eocene phase of upright 060°-trending F_3 folds accompanied by greenschist facies metamorphism.

INTRODUCTION

IN ALPINE Corsica, ophiolites of Jurassic age and their Lower Cretaceous oceanic sedimentary cover comprising the Schistes Lustrés (*sensu lato*) series (Durand-Delga 1978) have been obducted onto a Hercynian crystalline basement with Permian intrusives, locally covered by a Permian volcanoclastic series. The Schistes Lustrés nappes comprise imbricate lens-shaped units separated by ductile shear contacts which are assumed to have been subhorizontal before late phases of folding (Mattauer *et al.* 1981). The simplified geological map and cross sections of Cap Corse (see location map, Fig. 1) show that serpentinites, gabbros, metavolcanics, quartzites, marbles and calc-schists occur in an irregular succession (Figs. 2a–c). Deformation associated with nappe emplacement is accompanied by high P/low T metamorphism and has been considered to approximate to simple shearing (Mattauer & Proust 1975, 1976, Mattauer *et al.* 1977, 1981) of variable direction (Faure & Malavieille 1981).

The purpose of this paper is to describe the complex structures observed in Cap Corse formed during a progressive deformation event associated with nappe emplacement and followed by the superposition of three further deformation phases. Representative examples of structures in different lithologies are given.

The various rock types of Cap Corse have been mapped and described by Guillou (1962) and Primel (1963), and presented as the Luri 1:80,000 map sheet, simplified in Fig. 2(a).

Present-day orientations of field measurements are used throughout. For comparison with the rest of the Western Alps, one must take into account Corsica's 30° anticlockwise Oligo-Miocene rotation (Bellon *et al.* 1977).

* Present address: Geology Department, University of Western Australia, Nedlands, Western Australia 6009, Australia.

† This paper was presented at the meeting on 'Multiple deformation and foliation development' held in Bermagui, N.S.W., 4–11 February 1984. The revised manuscript was not available for inclusion in the special issue (7, 3/4) arising from the meeting.

STRUCTURES ASSOCIATED WITH OBDUCTION OF THE SCHISTES LUSTRES *s. l.*

Stretching-lineation trajectories

A stretching-mineral lineation, L_1, formed during blueschist-facies metamorphism is assumed to be parallel to the direction of maximum stretch of the finite-strain ellipsoid. Because of the high values of shear strain within the nappes, L_1 has been considered to be parallel to the shearing direction and hence provides the direction for nappe transport (Mattauer & Proust 1975, Mattauer *et al.* 1977, 1981, Faure & Malavieille 1981). Mapping of L_1 in the Schistes Lustrés (*sensu lato*) of Cap Corse has shown the existence of three distinct zones within which L_1 is of approximately constant orientation (Fig. 2c). Non-coaxial deformation criteria provide a shear sense towards the west in zone A, which is separated along a major thrust contact from the overlying zone B, where a constant, primary shear sense towards the south-southwest is observed. Though differing in orientation, primary structures associated with nappe emplacement are equivalent in both zones A and B. The author considers that eastwards-shearing (Malavieille 1983) in gneisses of zone C represents a back-thrusting of this klippe during second-phase deformation.

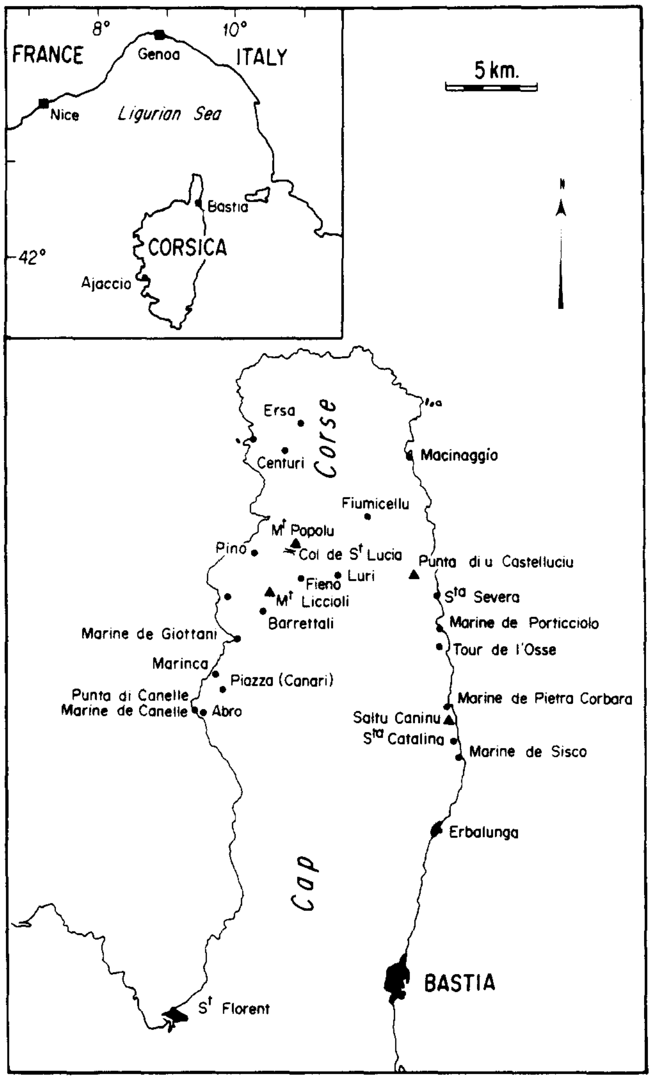

Fig. 1. Location map showing place names cited in the text.

First-generation structures in the different lithologies

Equal-area projections of representative first-generation structures are shown in Fig. 3. In Cap Corse, Mg-gabbros (often referred to as 'euphotides') are generally highly deformed and consist of relict pyroxenes (which may be partly altered to actinolite or recrystallized to metamorphic Na-pyroxenes) in a white to pale green epidote–actinolite–chlorite matrix. South of Punta di Canelle, a transition can be observed from a lens of practically undeformed gabbro through to gabbro ultramylonite (Fig. 4). Almost undeformed gabbros show a prominent cumulate layering, S_0, locally cut by micro-gabbro and dolerite dykes. The cleavage of primary pyroxene crystals is in places deformed by kink bands (Fig. 4e). Minor shear zones cross-cut the gabbro and displace dolerite dykes. A foliation in the gabbro is discernible only in the immediate vicinity of these shear zones. A little further south, S_0 is folded about tight to isoclinal 020°-trending folds containing a strongly developed axial-plane foliation, S_1 (Fig. 4b). Alternate layers are folded into class 1c and 3 profiles, which together approach a similar fold style.

The foliation is best developed in originally fine-grained layers where it may be highly schistose due to the presence of abundant chlorite and fine actinolite. S_1 contains a strong mineral lineation parallel to fold axes. Parallelism of S_0 with S_1 along isoclinal fold limbs results in a transposed foliation with the development of lenticular domains around fold hinges, within which S_0 is still discernible.

Where the foliation intensity increases, S_0 is no longer recognizable. The general aspect of this foliation (displayed by the majority of Cap Corse Mg gabbros) consists of deformed primary pyroxenes, partially or totally transformed to actinolite, in a white or pale green matrix of epidote, actinolite and chlorite (Fig. 4f). Pyroxenes are separated into fragments by displacement along their mineral cleavage planes (which in places are pulled apart with actinolite fibres recrystallizing between segments. Figs. 4f & g), or, elsewhere, are plastically deformed into retort shapes. The deformation of pyroxenes, as well as pressure shadows developed around pyroxene can be used to determine the global sense of shearing (Figs. 4f–h). Shear bands (Fig. 4d) generally make an angle of between 15 and 30° with S_1. Though in each zone the majority of shear bands show a constant sense of obliquity with S_1 (in agreement with the bulk shear sense), conjugate shear bands are also present locally.

Ultramylonites are developed along a thrust contact within gabbros (along which a slice of serpentinite is included) near Marine de Canelle (Fig. 1). Long (up to several centimetres) asymmetric pressure shadows of actinolite and, in some places, newly crystallized Na-pyroxene with chromite-rich cores occur around sporadic small remnant pyroxene crystals or iron-oxide grains and provide an excellent criterion for southwards shearing in zone B. The foliation shows perturbation caused by rotation of these inclusions in an otherwise 'pasty' matrix. Figure 5(a) shows that these crystals are locally rotated in an opposite sense: a 'backwards rotation' is observed where a former pyroxene (now completely altered to actinolite) is cut by a shear band.

In some ultramylonites, L_1 turns within the foliation and has different orientations from one layer to another. A probable continuation of this thrust contact (totally within gabbros, the serpentinite slice having lensed out) is seen on road-cuts on the road from Abro to Piazza (Fig. 1). Strain in this region is extremely inhomogeneous. In localized shear zones, secondary shear bands show a constant obliquity with S_1 in agreement with S-directed shearing. L_1 here shows a constant orientation to 026°. In one highly sheared zone, gabbro mylonites have been folded into sheath folds (Fig. 6a), whose axes are parallel to L_1 in unfolded layers: in places, L_1 is folded around sheath folds.

The association of extension fracturing and foliation boudinage with F_1 folding of the primary cumulate layering can also be seen along the above roadcuts. This is illustrated diagrammatically in Fig. 5(b). Here, parallel F_1 fold axes plunge gently to 195° within an axial-plane foliation dipping 24° to the west. Extension fractures

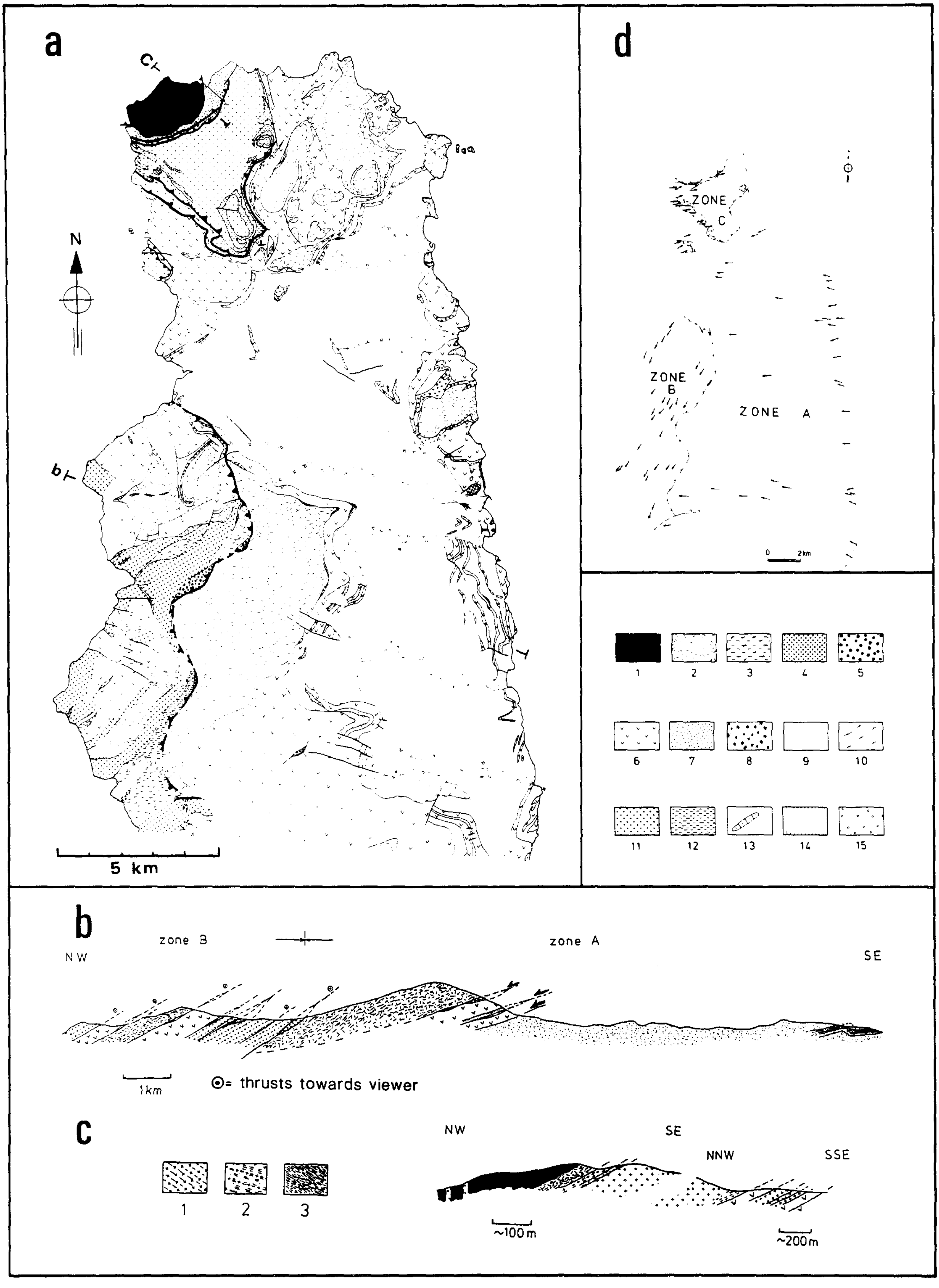

Fig. 2. (a) Simplified geological map of Cap Corse based on mapping by Guillou (1962) and Primel (1963). Modifications in the Ersa–Centuri area (zone C) after Malavieille (1983). 1, peridotite; 2, serpentinite; 3, undifferentiated basic and ultrabasic rocks; 4, Mg gabbro; 5, Fe–Ti gabbro; 6, prasinite and glaucophanite; 7, quartzite and quartz–mica schist; 8, gneiss and quartzite; 9, Schistes Lustrés *sensu stricto*; 10, phengite–glaucophane gneiss (Gneiss de Centuri); 11, Kinzigitic series (Ersa series); 12, amphibolite; 13, marble; 14, Cretaceous and Eocene sediments of Macinaggio; 15, scree and alluvium. Thrust contacts separate rock units; only major thrust contact between zones A, B, and C (Fig. 1d) are marked on the map. (b) Simplified cross-section of the area studied. (c) Left: contact of peridotites with gneiss; right: contact of South Alpine crust with ophiolites. 1, Mg gabbro; 2, prasinite derived from intense deformation of Mg gabbro; 3, schist derived from intense deformation of underlying gneiss. Directions of thrusting along contacts are shown. (d) Orientations of L_1 stretching lineations with arrowheads showing direction of overthrusting. The three zones are labelled A, B and C.

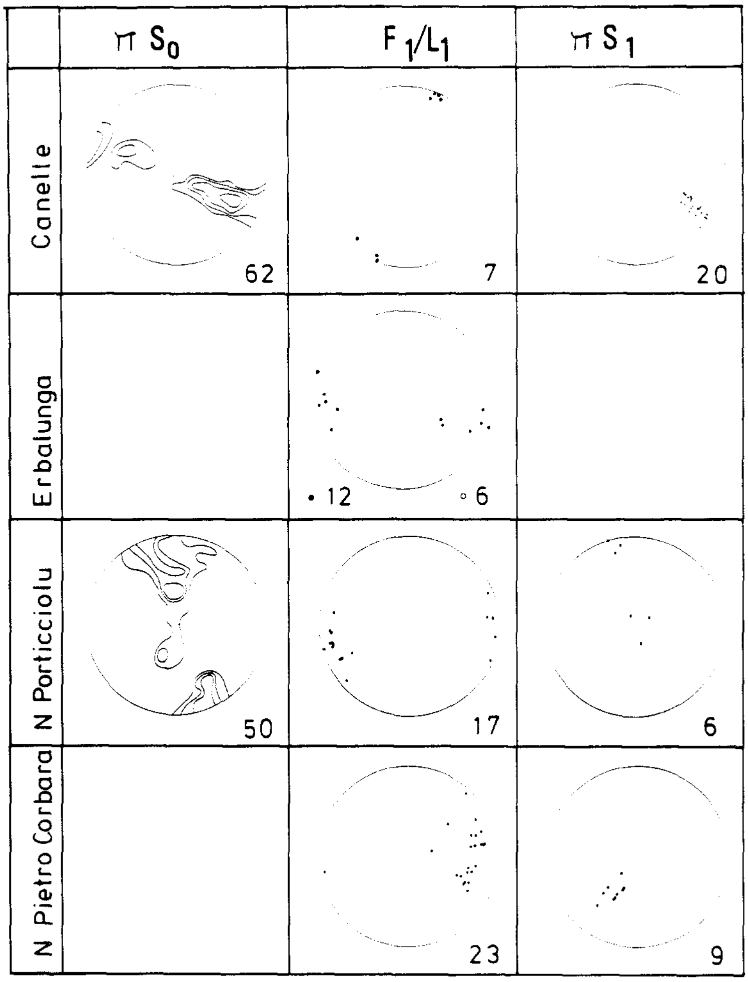

Fig. 3. Lower-hemisphere equal-area projections of first-phase structures. πS_0, poles to primary layering; F_1, F_1 fold axis (or L_1 at Erbalunga); πS_1, poles to first-phase (S_1) foliation. Canelle: folding of cumulate layering in Mg gabbros (zone B); Erbalunga: interstratified Mg and Fe–Ti gabbros (zone A). Closed circles: L_1; open circles, fibres of actinolite infilling fractures; north of Porticciolu and north of Pietro Corbara: Schistes Lustrés of zone A.

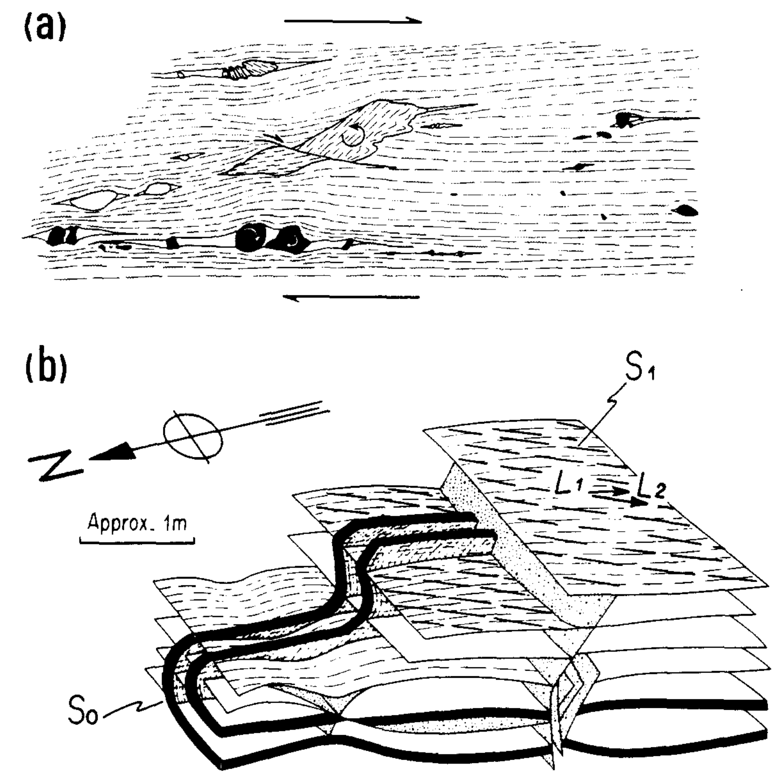

Fig. 5. (a) Interpretation of microstructures in a Mg gabbro mylonite. A former pyroxene (now almost completely transformed into actinolite) is displaced along a C′ shear band. The 'backwards rotation' of the upper pyroxene segment has perturbed the surrounding foliation in the matrix. Asymmetrical pressure shadows of actinolite are developed around both pyroxenes and opaques and may also be deformed by the rotation of irregularly shaped opaque grains (lower centre). (b) Formation of boudins, extension fractures and shear bands in a Mg gabbro. See text for details.

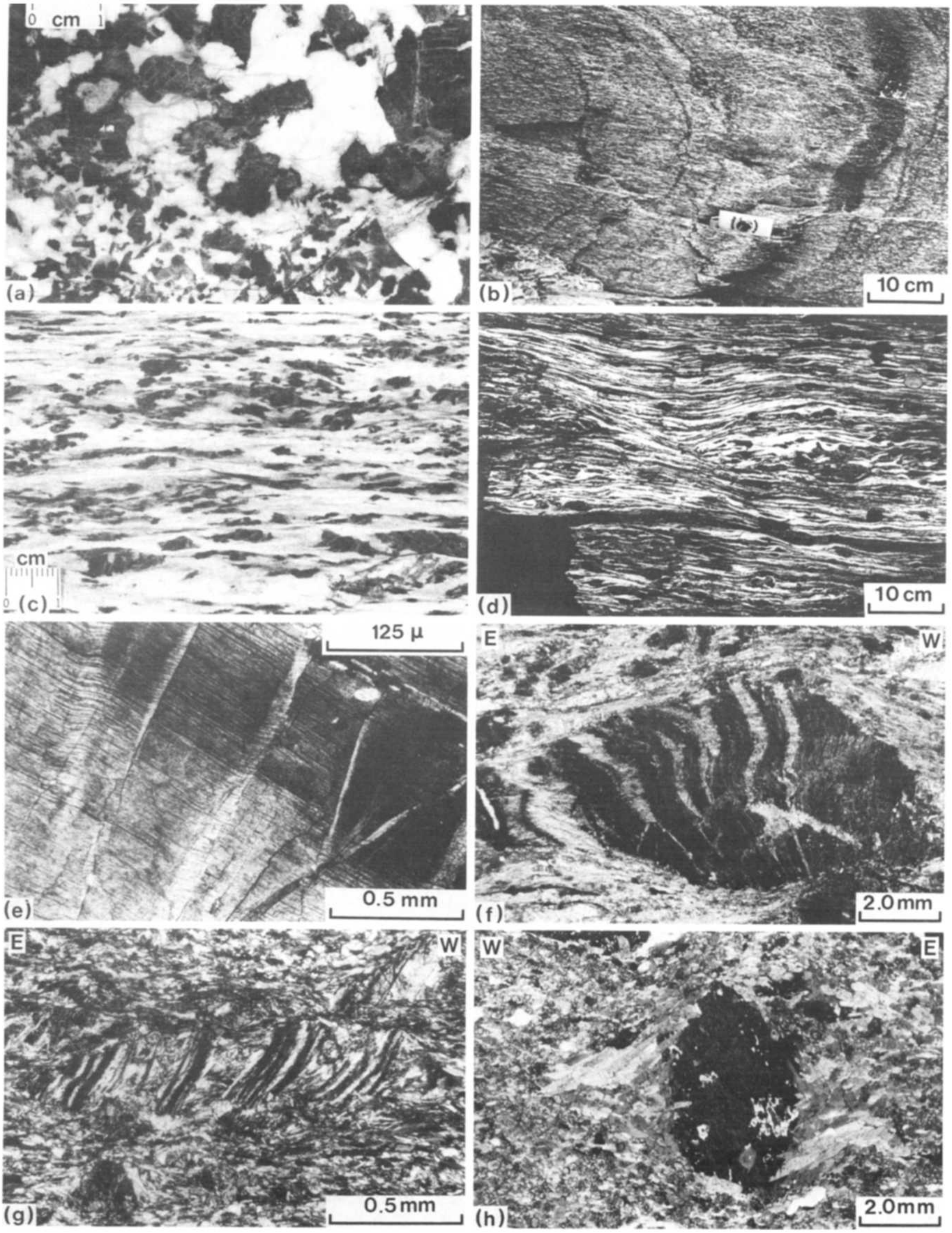

Fig. 4. Transformations from undeformed gabbros showing igneous textures to blastomylonites. (a) Detail of primary texture of almost undeformed Mg gabbros between the Marine di Canelle and Punta di Canelle. (b) S_1 foliation axial-planar to first-generation folds in a gabbro along the road between Piazza and Abro. (c) S_1 foliation in Mg gabbros where deformation is more intense. (d) Mylonitic Fe–Ti gabbro showing W-dipping C' shear band where L_1 is oriented E–W. (e) Kink bands affecting the mineral cleavage of a primary pyroxene in a macroscopically undeformed Mg gabbro. (f) Rotational fan-like opening of a primary pyroxene in a blastomylonitic gabbro. Actinolite has crystallized between segments. (g) Pull-apart of a primary pyroxene in which mineral cleavage planes are not suitably oriented for slip. (h) Crystallization of Fe-glaucophane and crossite in dissymmetric pressure shadows around chloromelanite in an Fe–Ti gabbro. The matrix of the rock is rich in garnet + glaucophane but garnet does not occur in pressure shadows.

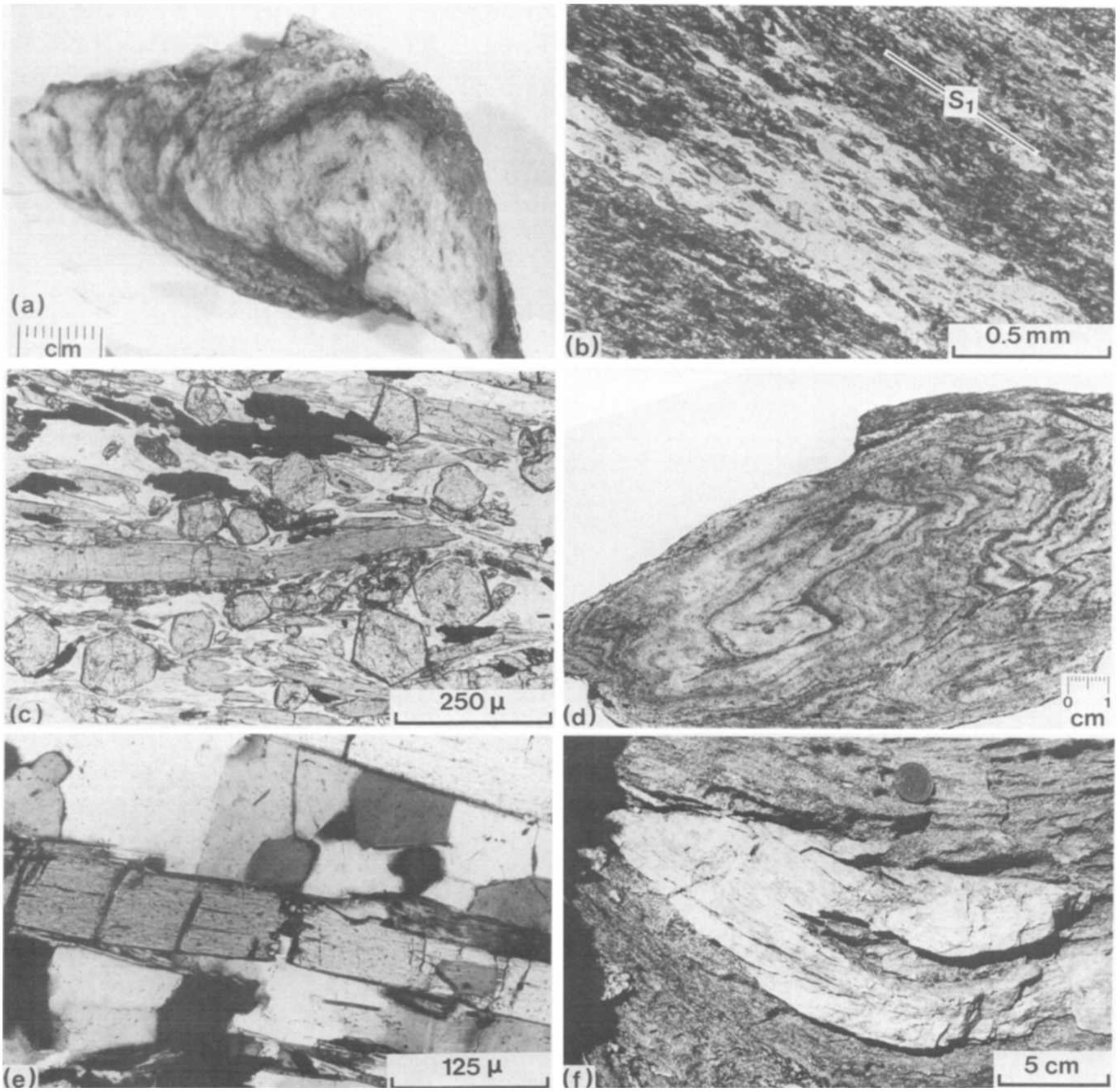

Fig. 6. (a) Sheath fold in Mg gabbro ultramylonite along a thrust contact between Piazza and Abro. Axes of sheaths are parallel to the regional orientation of L_1 (020°). (b) Foliation axial planar to isoclinal folds of epidote layering in a glaucophanite. (c) S_1 foliation (horizontal) in a garnet glaucophanite defined by the orientation of glaucophanes and epidotes. S_1 turns around garnets which are pre- or syntectonic. (d) Eye-shaped interference pattern in cross section perpendicular to the axes of sheath folds in quartzite layers in a micaceous quartzite from Piazza. The foliation within the micaceous quartzite matrix is horizontal, and is axial planar to isoclinal folds in the same outcrop as the sheath folds. (e) Fracturing of a glaucophane crystal in quartzite following a 'fibre-loading' model: the crystal initially fractured into two halves; these halves were separated during continuing deformation (with quartz infilling the resulting gap) and in turn they fractured midway along their lengths. This process continued until a critical limit is reached. (f) Marble layer in prasinites: note axial-plane cleavage enhanced by weathering. Also note thickening in hinge regions (between Sta Catalina and Saltu Caninu).

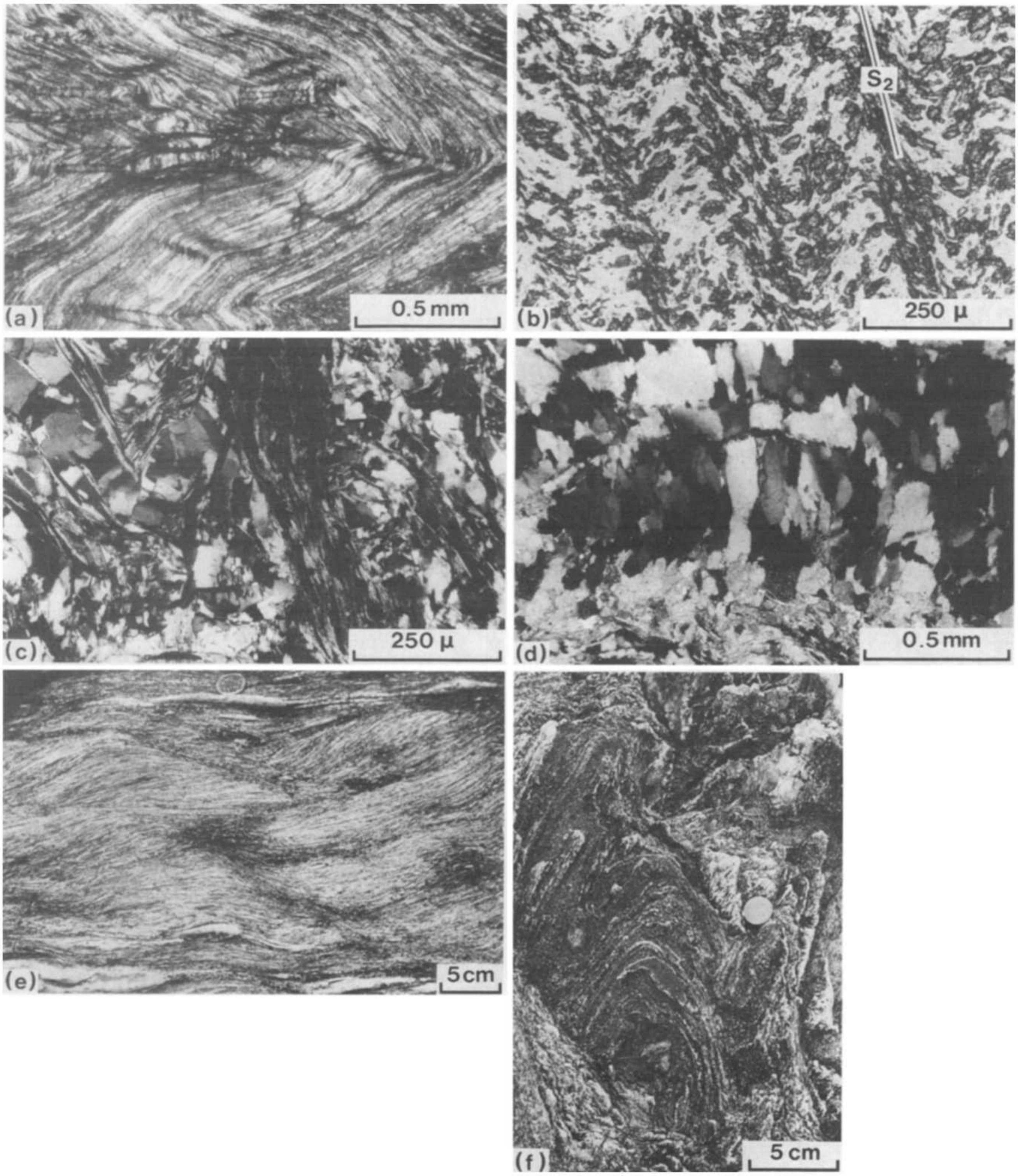

Fig. 8. (a)–(d). Second-generation microstructures. (a) F_2 microfold in gabbro mylonite showing a fine crenulation cleavage in the inner hinge zone (left of photograph). (b) Differentiated crenulation cleavage in a rodingite defined by the concentration of garnets in an antigorite + tremolite matrix. (c) Axial-plane differentiated crenulation cleavage in a quartz–mica schist. (d) Cleavage in the quartz-rich layers of (c), showing shape fabric of quartz grains whose long axes are parallel to S_2. (e) Shear bands in quartz–mica schist formed during the localized reutilization of S_1 foliation by SSW-directed shear east-northeast of Punte di u Castelluciu. (f) Sheath fold formed by late SSW-movement in a glaucophane-rich layer at the same locality as shown in (c).

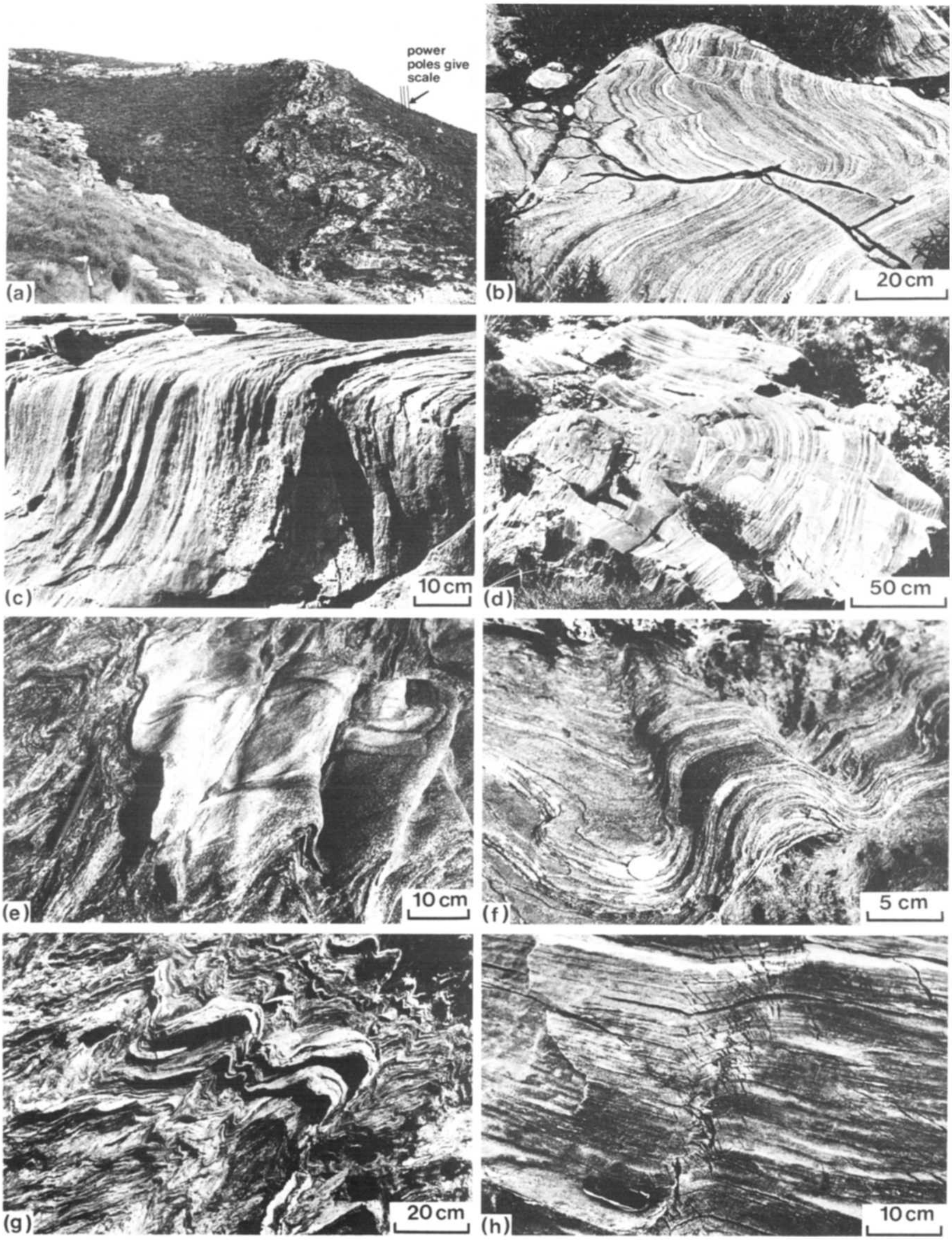

Fig. 9. F_2 and F_3 folds north of Santa Catalina. (a) General view of outcrops showing large-scale 'cascade' of F_2 folds in marble layers, overturned to the east. (b) F_2 folds in interbedded marbles and quartzites (detail of (a)). (c) Detail of 'knee-shaped' F_2 fold in marble showing the folding of a strongly developed L_1 lineation, which here is perpendicular to F_2. (d) Type-3 interference pattern in interbedded marble and quartzite. F_1 fold axes here have been reoriented towards parallelism with F_2 in the hinge of a large-scale F_2 fold. (e) Curving of F_2 fold axes in Schistes Lustrés (*sensu stricto*). Note large obliquity between the two fold hinges in the lower right-hand corner. (f) F_2 box fold. (g) Rounded hinges in quartz-calcite rich layers within mica-schists in F_2 folds. (h) F_3 folds in marble showing the formation of en échelon extension fractures along the axial plane.

making an angle of between 60 and 80° with L_1 cut the rocks. The foliation is also locally boudinaged: major S-dipping sigmoidal shear bands cut the foliation between boudins and turn to become parallel to S_1. Neighbouring layers show pinch-and-swell structures. Extension fractures and boudin-necklines elsewhere in both zones A and B also show a similar obliquity to the maximum stretching direction (represented by L_1 and the orientation of mineral fibres infilling fractures). The formation of these fractures may therefore be caused by failure along zones of localized plastic deformation similar to Lüders Bands as described by Burg & Harris (1982).

In prasinites and glaucophanites of both zones A and B, isoclinal and (rarely) sheath folds with S_1 axial planar (Figs. 6b & c) are defined by epidote-rich layers though, in general, epidote layering is parallel to S_1. An L_1 mineral-stretching lineation may be present, although this is commonly effaced by recrystallization associated with later deformation phases (see below). In some localities, ellipsoidal bodies probably representing former pillow lavas flattened in S_1 and elongated parallel to L_1 can be recognized in the prasinite series. In some exposures, S_1 is seen to turn asymmetrically around these objects.

First-phase deformation structures in the quartzite series, generally associated with prasinites (Primel 1963), are best seen by the village of Piazza (in zone B). Quartzite (chert) layers are folded into isoclinal and sheath folds (Fig. 6d). The S_1 foliation of interbedded quartz–mica schists, characterized by quartz ribbons (which have recrystallized to form a mosaic of individual quartz crystals showing triple-point junctions) separated by a planar orientation of phengites is axial planar to these folds. Shear bands are extremely well developed and present a constant sense of olibiquity with the foliation, S_1, implying here a shear sense towards the south-southwest. The foliation contains a strong stretching-mineral lineation trending north in which glaucophane crystals are fractured and pulled apart (Fig. 6e).

Grey–blue sericite schists with a characteristic brilliant or satinous lustre containing quartz nodules and exudates make up most of the Schistes Lustrés (*sensu stricto*) series. The schistosity is seen to be axial planar to rare mm- to cm-scale isoclinal folds of S_0 defined by quartz or carbonate layers, and contains a strong mineral-stretching lineation. Marbles and siliceous marbles with, near their contact with underlying prasinites, thin interbeds of prasinite occur at the base of the Schistes Lustrés (*sensu stricto*) series, especially along the east coast of Cap Corse in the vicinity of the Marine de Sisco (Fig. 1). First-generation folds (Fig. 6f) are isoclinal and show thickening of the hinge regions. Isoclinal folds in siliceous marble are of fold classes 1c, 2 and 3, whereas folds of isolated layers within prasinites (Fig. 6f) are folded into similar folds (class 2). Where marbles contain white micas and stilpnomelane, these minerals define an axial-plane S_1 foliation which, in siliceous layers, is accompanied by a change in quartz-grain fabric.

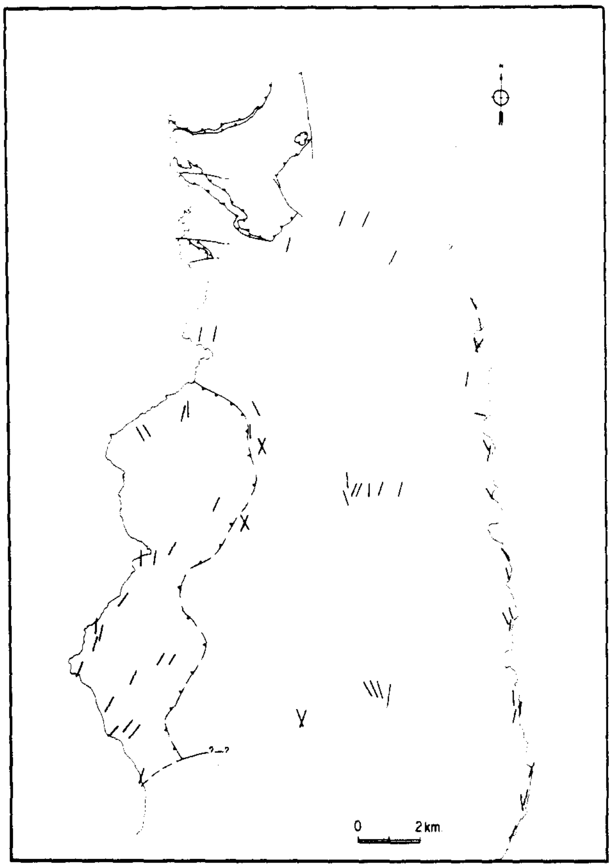

Fig. 7. Axial traces of second generation, F_2 folds (note that in detail, minor F_2 folds may show curved axes).

SECOND-GENERATION STRUCTURES

The S_1 foliation in both zones A and B is folded about a second generation of folds overturned towards the east and locally accompanied by minor E-directed thrusts.A map of the axial traces of F_2 fold axes is shown in Fig. 7. The nature of these structures differs with rock type.

Metre-sized F_2 folds which locally refold the S_1 foliation of Mg-gabbros are generally concentric folds with rounded hinges, generally trending north-northeast. An S_2 crenulation cleavage (Fig. 8a) is parallel to their W-dipping axial planes and is visible as a fine crenulation lineation, L_2, on S_1. Within zone B, second-generation folds are coaxial with, or at a slight angle to, first-phase folds, whereas in zone A the two generations are approximately perpendicular. F_2 fold axes are in places oblique to the maximum extension direction active during the second phase of deformation. Gabbros cropping out north of Erbalunga (Fig. 1, zone A) are folded about 020°-trending F_2 folds. However, actinolite fibre infill within oblique fractures indicates a maximum extension direction towards 350°.

Minor E-directed thrusts are associated with F_2 folds. Highly sheared gabbros along thrust contacts have been altered to prasinites. Near these contacts, small-scale F_2 folds, overturned to the east and generally trending towards 015°, have curved axes, and in the most highly deformed zones trend towards 110°.

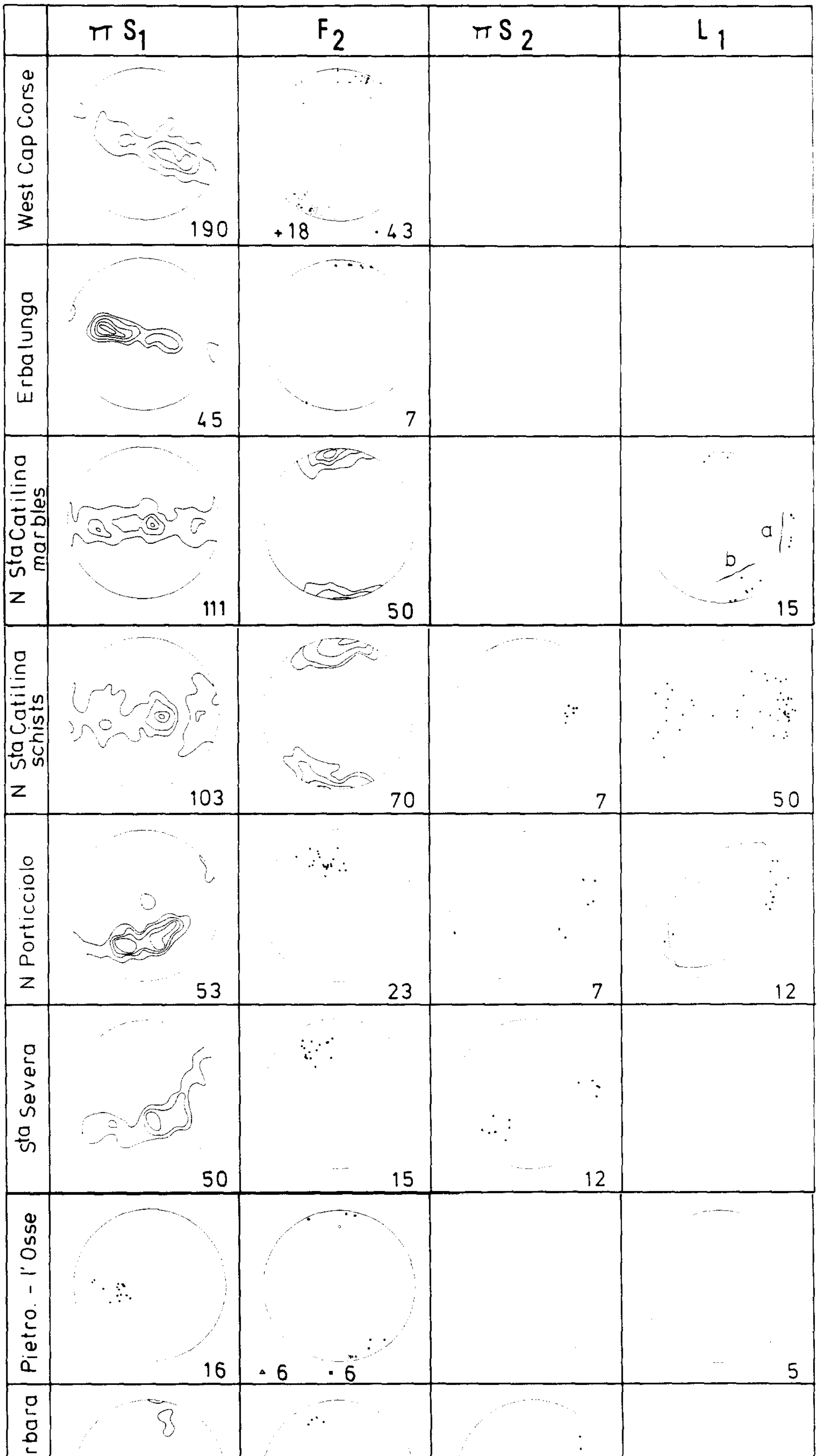

Fig. 10. Lower-hemisphere equal-area projections of second generation structures. πS_1, poles to S_1 foliation; F_2, second generation fold axes; πS_2, poles to axial planes of F_2 folds; L_1, orientation of first-phase lineation folded around F_2. West Cap Corse: Mg gabbros (total of measures from zone B): measures of L_2 and F_2 fold axes. Erbalunga: interstratified Mg and Fe–Ti gabbros. N. Sta Catalina marbles: a, general orientation of L_1 and F_1; b, reoriented L_1 and F_1 parallel to F_2 in the hinge of a major second generation fold. N. Sta Catalina schists: note great dispersal of L_1. N. Porticciolo Schists: L_1 is distributed about a great circle with β close to orientation of F_2. Sta Severa: glaucophanites and prasinites. Pietro-l'Osse: schists between Pietrocorbara and the Tour de l'Osse. N. Pietrocorbara: Schistes Lustrés.

In rodingitized dykes within serpentinites (representing the metasomatic greenschist ocean-ridge metamorphism of gabbroic dykes in a peridotite) an S_1 foliation defined by garnets and serpentine parallel to the dyke-wall contact is crenulated by F_2 layering in which garnet is extremely abundant. Where there is a higher percentage of serpentine, this cleavage changes to a differentiated crenulation cleavage where garnets are concentrated as microlithons along the steeper limb of disymmetric crenulations (Fig. 8b). This cleavage is seen to turn towards parallelism with the serpentinite host-rock, possibly implying that shearing took place along this interface.

Prasinites between Marine de Pietra Corbara and Tour de l'Osse (Fig. 1) show some of the complexities associated with F_2 folding. Here, prasinites are folded by recumbent folds whose axes are variable in orientation, even between neighbouring folds, and whose axes in places are curved. Two prominent orientations of F_2 exist: 05° towards 005° and 07° towards 150°. Parasitic folds also show divergent fold axis orientations. An L_2 crenulation lineation either bifurcates to parallel both fold orientations or makes an oblique angle with the F_2 fold axis.

Second-generation 'cascade' folds can be seen in bands of marble and siliceous marble within zone A north of Santa Catalina (Fig. 9a). Major fold hinges are open, rounded (Fig. 9b) or 'knee-shaped' and plunge gently to between 330 and 020°, with a maximum towards 350°. Minor parasitic F_2 folds are of variable orientation and generally die out rapidly along axis or merge with neighbouring folds, whereas major F_2 folds are cylindrical and may be followed for long distances. Folds show a variation in style from class 1c to 3. F_1 folds approximately perpendicular to F_2 are clearly refolded by F_2 (Fig. 9c) in most localities; however, in the hinge of some major F_2 folds, isoclinal F_1 folds have been rotated towards parallelism with F_2, producing a type-3 interference pattern (Fig. 9d). In the example shown in Fig. 9(d), glaucophane crystals defining L_1 also show a reorientation towards parallelism with F_2. In quartz-mica schists in siliceous marbles, a strongly differentiated crenulation cleavage is parallel to S_2 axial planes (Fig. 8d). In quartz layers, S_2 is defined by pressure solved quartz crystals (Fig. 8a).

Typical F_2 folds within the Schistes Lustrés (*sensu stricto*) are shown in Figs. 9(e–g). Schists, including some interbedded within limestone or quartz-rich layers, are folded into tight chevron folds, some of which have slightly rounded hinges, or into box folds. Interbedded quartz- or calcite-rich layers form more rounded fold profiles. Fold hinges are commonly curved and show plunge variations. Folds die out along plunge and anticlinal terminations of one fold may merge with a neighbouring syncline. Isoclinal F_1 folds and L_1 lineations are folded about F_2; fold styles in these strongly foliated rocks are characteristic of flexural-slip folding.

Orientation of second generation structures

The orientation of F_2 folds in schists (Fig. 10) varies slightly about a general attitude of being overturned to the east with axial planes dipping between 40 and 50° to the west. Fold axes have an extremely wide variation in plunge and azimuth with the mean plunge gentle towards 020°. Refolded L_1 shows a great dispersal about F_2 folds. Further north, beyond the north side of Porticciolo Bay, F_2 folds refold abundant F_1 folds. F_2 folds here have steeper north-northwest plunges and steep W-dipping axial planes.

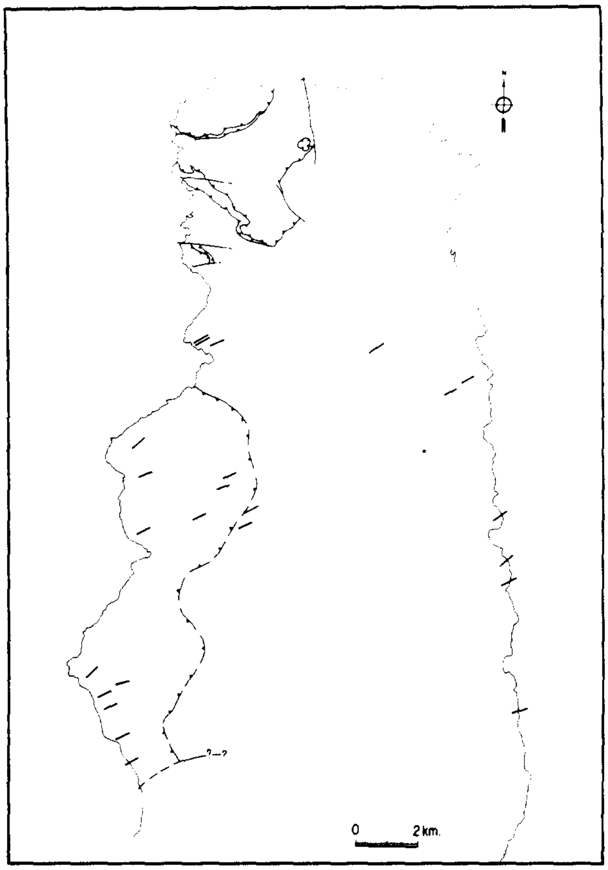

Fig. 11. Orientation of F_3 fold axes.

Summary

The second deformation event in the Schistes Lustrés of Cap Corse is characterized by E-verging folds of variable style (which depends upon the lithology) and an associated crenulation cleavage. Fold axes vary from NNE to NNW orientations with maxima towards either 020 or 330°. Minor E-directed thrusts accompanying F_2 folds have been seen within zone B. In such outcrops, F_2 folds are of variable orientation and exhibit a tendency towards parallelism with the E-directed thrusts in the most-deformed zones. Second-generation structures are considered to be contemporaneous with the E-backthrusting of the higher-level Ersa–Centuri klippe in Northwest Cap Corse (Caby *et al.* in press).

It is not possible to state whether the reorientation of F_1 isoclinal folds towards parallelism with F_2 occurred during the F_2 folding, or if this local reorientation is due primarily to the change in direction of first-phase thrusting of zone B locally affecting the underlying series of zone A, is discussed further below.

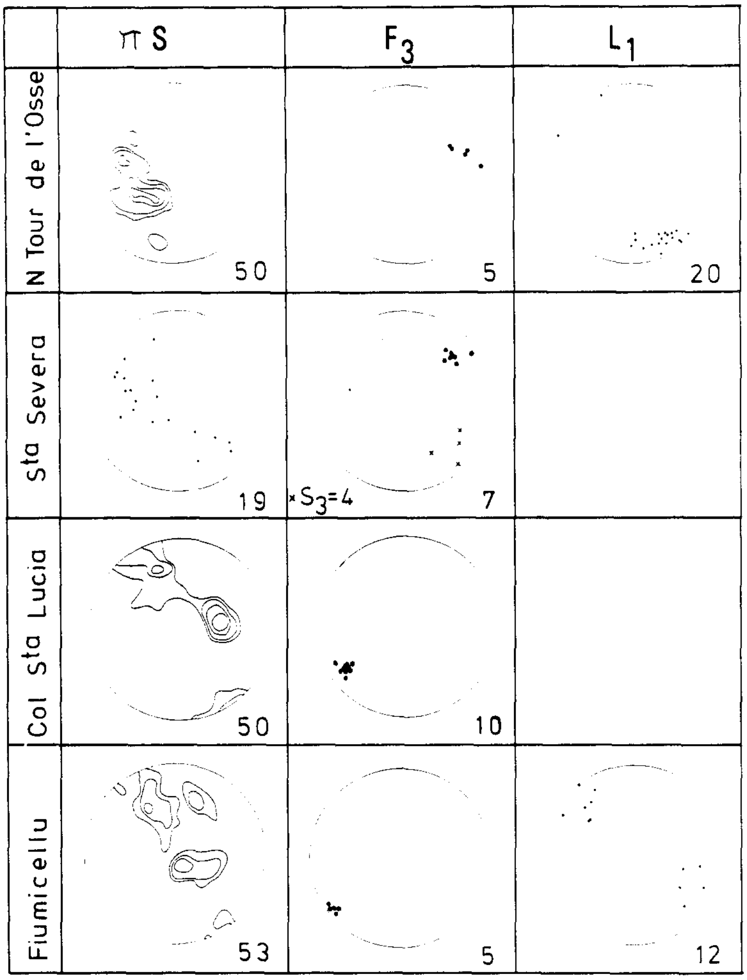

Fig. 12. Lower-hemisphere equal-area projections of structural data in areas of F_3 folding. N Tour de L'Osse: prasinites. Sta. Severa: glaucophanites and prasinites, also showing poles to S_3 axial planes (crosses). Col de Sta. Lucia: Schistes Lustrés. Fiumicellu: Schistes Lustrés. πS_1, F_3 and L_1 as in Fig. 10.

THIRD-GENERATION STRUCTURES

A third fold generation is recognized locally refolding or overprinting F_1 and F_2 structures. F_3 folds are best developed in prasinites and schists though other lithologies are also affected locally. A map illustrating trends of F_3 fold axes is shown in Fig. 11, and orientations of structures in areas of F_3 folds are shown in Fig. 12.

Very finely foliated actinolite–chlorite schists formed from Mg gabbros along some major first-generation thrust contacts may contain an L_3 crenulation trending towards approximately 060° in both zones. In gabbros along the west coast (zone B), a mineral lineation defined by the alignment of albite crystals ± sericite ± chlorite is parallel to the L_3 crenulation. Prasinites here show an extremely well-developed mineral lineation (especially defined by mm-sized albite crystals) trending approximately 060°, which in places is the only lineation clearly visible in the rock. In earlier studies describing 'E–W lineations', this lineation was probably interpreted as being associated with the first-phase deformation. In prasinites and glaucophanites cropping out along the ridge in the vicinity of Mt Liccioli (Fig. 1), S_1 contains a strong 060° lineation, in part a mineral lineation as described above, and in places paralleled by an additional faint crenulation. Some cm-sized isoclinal fold hinges within a transposed foliation of the thin alternating glaucophane and epidote layering can be recognized. These F_1 folds plunge gently towards 025°. In prasinites higher in the series (near a thrust contact with serpentinites) metre-sized chevron-style folds plunge 15° towards 060° with axial planes dipping south-southeast at 65°, and refold S_1 and an L_1 mineral lineation trending between 190 and 210°. It is therefore clear that the 060°-lineation is a third-generation structure acquired during folding contemporaneous with greenschist-facies metamorphism, during which the prasinites were the most susceptible rock type for recrystallization.

Prasinites of zone A are much less affected by F_3 folding, and, where such folds do occur, their extent is extremely limited. F_3 folds plunging between 060 and 070° on the limb (dipping approximately 45° to ENE) of a large F_2 fold are seen north of the Tour de l'Osse. These folds clearly refold an L_2 crenulation lineation and are accompanied by an axial-plane S_3 crenulation cleavage. F_3 folds of cm- to m-wavelength, generally of chevron style, affect glaucophanites and especially overlying prasinites and schists in a limited area of coastal outcrop south of Santa Severa (Fig 1). Centimetre-scale microfolds in glaucophanite have great variation in style: kinks, box folds and open folds with rounded profiles affect isolated layers only, dying out in a short distance along their axial planes. F_3 folds plunge at approximately 25° towards an azimuth between 045 and 055°, with axial planes dipping at between 60 and 80° towards the northwest.

Rare F_3 folds in marbles are characterized by the association of minor folds with brittle deformation structures: en échelon extension fractures occur along the axial planes of F_3 flexures plunging gently between 060 and 070° (Fig. 9h).

F_3 folds in schists are extensively developed in the north of the area studied. Roadcuts southeast of Mt Popolu (Fig. 1) show the superposition of F_3 folds plunging 15° towards 235° on both limbs of tight to almost isoclinal m-sized F_2 folds of E-vergence, plunging at 06° towards 330°. At Fiumicellu, 055°-trending F_3 folds refold an earlier mineral lineation parallel to cm-sized isoclinal folds. Here, S_3 axial planes dip at approximately 55° to the northwest.

FOURTH-GENERATION LARGE-SCALE FOLDING

The present-day predominent attitude of the Schistes Lustrés (*sensu lato*) (prominent steep W dips of S_1 in western Cap Corse and gentler E dips on the eastern side of the Cap) is caused by a major N–S anticline (whose axis is offset to the east of the central mountain ridges, Durand-Delga 1978). This anticline also separates allochthonous units of identical origin at St Florent and Macinaggio (Fig. 1).

EFFECTS OF THRUSTING OF THE NAPPES OF ZONE B ONTO THE UNDERLYING SERIES OF ZONE A

As described above, equivalent structures associated with first-phase deformation are found in both zones A and B; only their orientations differ between the two zones. However, ophiolites directly below the thrust contact separating zones A and B (as seen west of Fieno, Fig. 1) and also within the underlying nappes initially emplaced towards the west (the most northerly outcrop of which is on the coast east-northeast of Punta di u Castelluciu) may in places have been affected by the thrusting of the uppermost series towards the south-southwest. In these areas, the following sequence of events is deduced.

(1) Initial W-directed thrusting of zone A contemporaneous with high P/low T metamorphism is responsible for the S_1 foliation containing an E–W mineral-stretching lineation, L_1, and E–W trending isoclinal folds.

(2) The series was affected by inhomogeneous SSW-directed shearing producing: (a) localized shear zones—S_1 appears to have been utilized by SSW-directed shearing or in places is cut by shear bands on a decimetric scale dipping to the south-southwest (Fig. 8e); (b) a stretching lineation trending to approximately 015°; (c) reorientation of L_1, especially of large glaucophane needles and many previously formed isoclinal folds towards parallelism with the new stretching direction, L_1, (i.e. second shear direction) within S_1; (d) sporadic folding of S_1 about isoclinal microfolds parallel to L_1 or the formation of sheath folds (with the refolding of L_1 about these structures; Fig. 8f); (e) possible recrystallization of small glaucophane crystals parallel to L_1—implying the persistence of high P/low T metamorphic conditions during SSW-directed shearing.

(3) Second-generation folds and kink bands refolded all these structures.

TIMING OF DEFORMATION EVENTS

High P/low T metamorphism contemporaneous with first-phase deformation has been dated at 100–80 Ma by $^{39}Ar/^{40}Ar$ (Maluski 1977) and Rb/Sr methods (Cohen *et al.* 1981). In Corsica, evidence that obduction had terminated by the Palaeocene is given by the inclusion of pebbles containing minerals of high P/low T paragenesis within Lower Eocene conglomerates (Amaudric du Chaffaut 1982). Detrital ferroglaucophane has been found in turbidites interbedded with Maestrichtian outer-shelf marls in eastern Sardinia, the source of which is thought to be a southwards continuation of the Alpine Corsican orogen off the eastern coast of Sardinia (Dieni & Massari 1982).

The second deformation phase is of probable Middle to Late Eocene age as further south in Corsica, the Eocene is affected by a second-generation cleavage (Sauvage-Rosenberg 1977) probably equivalent to S_2 in Cap Corse.

From a microtectonic study of brittle deformation structures in neighbouring Sardinia, Letouzey *et al.* (1982) inferred a 140°-trending principal compression direction affecting sediments of probable Middle Eocene age (conglomerates containing Cuisian–Lutetian material) as well as Cretaceous and Jurassic limestones. Minor monoclinal axes also occur locally, approximately perpendicular to this compression direction, and are considered to have been contemporaneous with the brittle deformation (Letouzey *et al.* 1982). These authors attribute this compression direction to an Upper Lutetian to Late Eocene deformation phase predating Corsica and Sardinia's 30° anticlockwise rotation. Burdigalian compression directions show the same orientation in Sardinia as in other areas of the Western Mediterranean (therefore rotation terminated in the Early Miocene), whereas the 140° compression makes an angle of approximately 30° with compression directions of comparable age in the Western Mediterranean. As F_3 fold axes in Corsica are approximately perpendicular to the 140° compression direction, the third generation of structures can be considered contemporaneous with the above structures described in Sardinia. Fission-track data (Carpena *et al.* 1979) indicate an important metamorphic event of Late Eocene age, previously considered to have been contemporaneous with the second-phase deformation (Mattauer *et al.* 1981). As F_3 folds are accompanied by a very strong greenschist-facies metamorphism, a Late Eocene age for this event is therefore in agreement with both microtectonic and fission-track data.

Fourth-phase folding is inferred to be of Late Miocene to Quaternary age as Miocene sediments near St Florent are affected by a major syncline alongside the Cap Corse anticline.

IMPLICATIONS FOR THE STUDY OF MULTIPLY DEFORMED TERRAINS

It is important to note the difficulty in relating the different macro- and micro-structures to a given deformation event on the basis of style or orientation. It is clear that style and development of structures vary greatly between different rock types and that attention must be paid to the metamorphic assemblages defining each mineral lineation. During a single phase of progressive non-coaxial deformation due to thrusting, the maximum stretching direction (and orientation of structures such as stretching lineations and isoclinal fold axes parallel to this direction) can be shown to vary in a continuous manner or to be discontinuous, as described above in Cap Corse, where there are two areas in which primary structures differ in orientation. Where the direction of nappe emplacement changes with time, earlier-formed structures may be deformed by shearing towards the new shear direction. Here, the idea of distinct deformation phases cannot be applied as the localized superposition of structures takes place within a continuous progressive deformation event (see Brun & Choukroune 1981), associated with ophiolite obduction under the same prevailing high-pressure metamorphic conditions. Difficulties in interpretation are brought about by the local reorientation towards the new stretching direction of passive markers, such as glaucophane needles defining a primary lineation.

Acknowledgements—Many thanks are due to J. P. Burg, D. Gapais and C. McA. Powell for improvements to the original manuscript.

REFERENCES

Amaudric du Chaffaut, S. 1982. Les unités alpines à la marge orientale du massif cristallin corse. *Trav. Labor. Géol.* **15**. Ecole Norm. Sup., Paris.

Bellon, H., Coulon, C. & Edel, J. P. 1977. Le déplacement de la Sardaigne: synthèse des données géochronologiques, magmatiques et paléomagnetiques. *Bull. Soc. géol. Fr.* **119**, 825–831.

Berthé, D., Choukroune, P. & Jegouzo, P. 1979. Orthogneiss, mylonite and non-coaxial deformation of granites: The example of the South Armorican Shear Zone. *J. Struct. Geol.* **1**, 31–42.

Brun, J. P. & Choukroune, P. 1981. Déformation progressive et structures crustales. *Rev. Géogr. phys. Géol. dyn. Paris* **23**, 177–193.

Burg, J. P. & Harris, L. B. 1982. Tension fractures and boudinage oblique to the maximum extension direction: an analogy with Lüders Bands. *Tectonophysics* **83**, 347–363.

Caby, R., Kienast, J. R., Harris, L. B. & Guiyaud, M. in press. Les klippes de socle anté-alpin du Cap Corse: arguments pétrogénetiques et géometriques pour une origine sud-alpine. *Bull. Soc. géol. Fr.*

Carpena, J., Mailhé, D., Naeser, C. W. & Poupeau, G. 1979. Sur la datation par traces de fission d'une phase tectonique d'âge Eocène Supérieur en Corse. *C. r. hebd. Séanc. Acad. Sci., Paris* **289**, 289–292.

Cohen, C., Schweickert, R. A. & Odom, L. 1981. Age of emplacement of the Schistes Lustrés Nappe, Alpine Corsica. *Tectonophysics* **73**, 267–283.

Dieni, I. & Massari, F. 1982. Présence de glaucophane détritique dans le Maastrichtien inférieur de Sardaigne orientale. Implications géodynamiques. *C. r. hebd. Séanc. Acad. Sci., Paris* **295**, 679–682.

Durand-Delga, M. 1978. La Corse, In: *Géologie de la France, Volume 2* (edited by Debelmas, J.). Doin, Paris, 465–478.

Faure, M. & Malavieille J. 1981. Etude structural d'un cisaillement ductile: le charriage ophiolitique corse dans la région de Bastia. *Bull. Soc. géol. Fr.* **23**, 335–343.

Guillou, J. J. 1962. Etude géologique et métallogénique de la partie septentrionale du Cap Corse. Thèse 3[e] Cycle, Université de Paris.

Letouzey, J., Wannesson, J. & Cherchi, A. 1982. Apport de la microtectonique au problème de la rotation du bloc corsosade. *C. r. hebd. Séanc. Acad. Sci., Paris* **294**, 595–602.

Malavieille, J. 1983. Etude tectonique et microtectonique de la nappe de socle de Centuri (zone des Schistes Lustrés de Corse); conséquences pour la géométrie de la chaîne alpine. *Bull. Soc. géol. Fr.* **25**, 195–205.

Maluski, H. 1977. Application de la méthode $^{39}Ar/^{40}Ar$ aux minéraux des roches cristallines perturbées par les événements thermiques et tectoniques en Corse. Thèse Sci., Université de Montpellier.

Mattauer, M., Faure, M. & Malavieille, J. 1981. Transverse lineation and large-scale structures related to Alpine obduction in Corsica. *J. Struct. Geol.* **3**, 401–409.

Mattauer, M. & Proust, F. 1975. Donnés nouvelles sur l'évolution structurale de la Corse alpine. *C. r. hebd. Séanc. Acad. Sci., Paris* **281**, 1681–1684.

Mattauer, M. & Proust, F. 1976. La Corse alpine: un modèle de genèse de métamorphisme haute-pression par subduction de croûte continentale sous du matériel océanique. *C. r. hedb. Séanc. Acad. Sci., Paris* **282**, 1249–1252.

Mattauer, M., Proust, F. & Etchecopar, A. 1977. Lineation 'a' et mécanisme de cisaillement simple lies au chevauchement de la nappe des Schistes Lustrés en Corse. *Bull. Soc. géol. Fr.* **19**, 841–847.

Primel, L. 1963. Etude géologique et métallogénique de la partie méridionale du Cap Corse. Thèse 3[e] Cycle, Université de Paris VI.

Sauvage-Rosenburg, M. 1977. Tectonique et microtectonique des Schistes Lustrés et ophiolites de la Vallée du Golo (Corse Alpine). Thèse 3[e] Cycle, Université de Montpellier.